Micro-wire Pirani with temperature-stabilized Environment

Rahiman, M. Fuad; Berndt, Dominik; Schreiner, Rupert
Ostbayerische Technische Hochschule Regensburg
https://doi.org/10.57688/361

Abstract

We present a Pirani vacuum gauge with an actively temperature-stabilized environment. The heated sensor element is surrounded by two elements that are temperature-controlled to a certain level below the temperature of the heated sensor element. The idea is to create a homogeneous temperature distribution, which allows keeping the ambient temperature constant, thus increasing the accuracy and repeatability of vac-uum measurements.

1. Introduction

Vacuum sensors play a crucial role in the semiconductor manufacturing industry. Several processes such as plasma deposition, plasma etching [1], physical vapor deposition [2], and scanning electron microscopy [3] have to rely on the accuracy and reliability of vacuum sensors to ensure a high quality of manufactured products. Among the various types of vacuum sensors in the current market, thermal conductivity vacuum sensors, called Pirani vacuum gauges, are widely used from high to rough vacuum. Pirani vacuum gauges are known for their reliability, low cost, and wide measurement range [4].

However, these sensors are very sensitive to small changes in ambient temperature which cause a drift of the sensor signal over time [5,6]. A few approaches have been demonstrated to address this issue, such as using dummy resistors [7,8], dual compensating resistors [9], or active substrate cooling [7].

In this work, we will present a new approach to minimize the drift in the ambient temperature around the Pirani sensor. Using active temperature stabilization in the form of constant temperature thermal gas interaction elements, a significant reduction of temperature-induced signal fluctuations of up to 83 % is achieved.

1.1. Working principle of miniaturized Pirani sensors

Pirani vacuum gauges use a heated sensor element, which can be a filament [10], a micro-wire [11], or a metal resistor film deposited on a thin membrane [7,8,12].

There are a few common operation modes of Pirani vacuum gauges such as pulsed mode, constant current (CC) mode, and constant temperature (CT) mode. The most

common mode of operation is the CT mode, since it has the advantage of higher sensitivity and a wider measurement range [13]. Here, the temperature of the heated sensor element is kept constant over the entire pressure range. This can be realized with a suitable circuit that controls the power required to maintain this constant temperature difference. The power P_H represents the measuring quantity and can be used to calculate the thermal conductance G_{th}:

$$P_H = G_{th} \bullet \Delta T = (G_G(p) + G_S + G_R) \bullet \Delta T \quad (1)$$

The calculated thermal conductance consists not only of the thermal conductance through the surrounding gas $G_G(p)$ but also of undesired thermal conductances through the solid connections G_S and radiation G_R. G_S and G_R can be combined as parasitic heat losses because they are not pressure-dependent and therefore reduce the sensitivity of the sensor.

In addition to the parasitic heat losses, the measurement output of a Pirani vacuum gauge is influenced by the ambient temperature T_{amb} as the heater power is directly proportional to $\Delta T = T_H - T_{amb}$. Since ambient temperature is not constant and depends on various factors like room ventilation and the presence of heat sources, even small temperature variations can cause a drift of the sensor signal affecting the accuracy and repeatability of a Pirani vacuum gauge.

2. Device design and concept

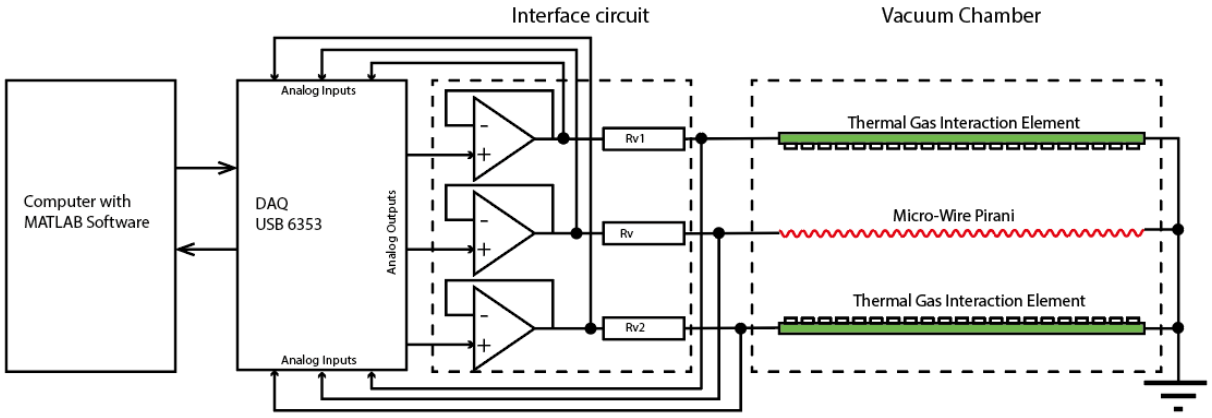

Fig. 1: Schematic diagram of the micro-wire Pirani device with thermal gas interaction elements and control circuit for electrical operation

By stabilizing the temperature around the sensor element, one could eliminate the influence of the fluctuations of the outer ambient temperature and minimize the long-term drift of the sensor measurement.

In this study, we use a micro-wire Pirani vacuum gauge. The sensor element is represented by a thin helix-shaped wire of tungsten. The wire has a diameter of 8 µm, the

winding radius is 50 µm, and is fixed between two pins of a TO-Socket. The temperature coefficient of resistance (TCR) of the micro-wire is 0.0074 K^{-1}.

For active temperature control, thermal gas interaction elements are arranged around the micro-wire. These elements are based on a 90 µm thick ZrO_2 substrate. These elements contain metallic heater structures, which are patterned by photolithography and metallized by physical vapor deposition. The TCR is 0.0016 K^{-1}. The thermal gas interaction elements are fixed below and above the helix-shaped wire with a distance of around 850 µm to the wire.

Fig. 1 shows a schematic design of the Pirani vacuum gauge including micro-wire and two thermal gas interaction elements and the digital CT operation setup.

To create a stable ambient temperature around the micro-wire Pirani, the temperature of both thermal gas interaction elements is kept constant by using a CT mode operation principle. The CT operation used in this work is a digital CT mode, where the output voltage regulation is done through a PID controller in a computer.

The interface circuit consists of an operational amplifier TLV2772A and a resistor to create a voltage divider between the resistance R_v, R_{v1}, and R_{v2}, and the micro-wire Pirani and both thermal gas interaction elements. The voltage across the sensor and thermal gas interaction elements will be recorded by the computer with a code written in MATLAB. The code calculates the difference between the actual and the desired temperature according to the PID method and returns a voltage output through the analog output of the DAQ module. The repetition rate of this PID control is 2000 loops per second and the temperature of all three device components can be regulated simultaneously while a measurement is performed.

The sensor device is placed in a vacuum chamber. The pressure range of the vacuum chamber is from $2 \cdot 10^{-7}$ mbar to atmospheric pressure and the pressure level can be controlled by the computer.

3. FEM-Simulations

A FEM-simulation in COMSOL Multiphysics is used to visualize the comparison of the temperature profile in the device with and without temperature stabilization. The ambient temperature is varied from 16°C to 24°C and the temperature profile along the z-axis between the two thermal gas interaction elements (see Fig. 2a) is calculated at atmospheric pressure.

Fig. 2(b) shows the temperature profiles without temperature stabilization whereas Fig. 2(c) shows the temperature profile while the temperature of thermal gas interaction elements is set at 25°C.

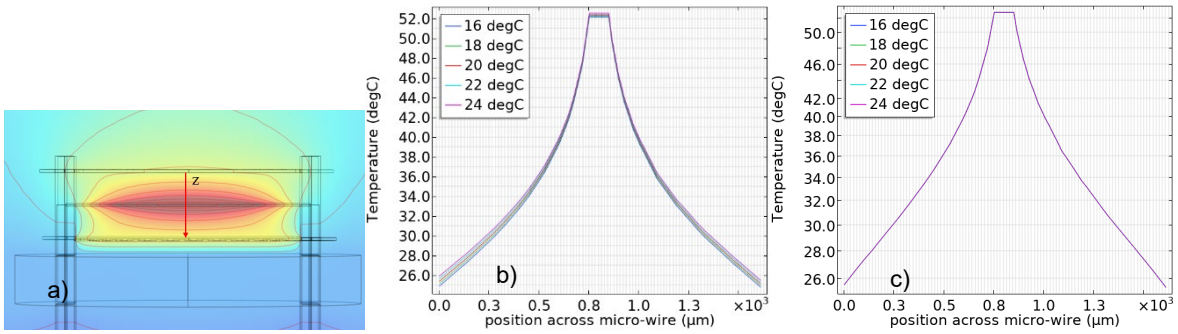

Fig. 2: Simulation of temperature profile across the z-axis (a) of the micro-wire Pirani with thermal gas interaction elements for b) without temperature stabilization and c) with temperature stabilization

Without temperature stabilization, the temperature deviates around 0.05°C at the center of the micro-wire and 0.1°C at the edge of the thermal gas interaction elements for every 1°C change in ambient temperature. On the other hand, the temperature profile of the device with temperature stabilization set to 25°C shows no deviation at all.

The drift in temperature on the micro-wire and the gas surrounding it will affect the measurement output as suggested in Eqn. 1, where the dissipated power at the sensor is directly proportional to the difference of the sensor temperature and the ambient temperature. According to the simulation, if a sensor is operated at 50°C, an ambient temperature deviation of 1°C will cause a 0.1 % deviation in the measured output power without temperature compensation.

4. Results and discussion

4.1. Sensor power versus temperature of the thermal gas interaction elements

Due to the heat exchange between the three heating components, a suitable operating temperature of the thermal gas interaction elements must be determined to ensure a stable operation of the system. This is done by studying the relationship of sensor power P_S versus varying thermal gas interaction elements temperature T_0. The stability of the PID control during the study is also monitored.

Using the device setup described in Sec. 2, the relationship between the sensor power P_S and the temperature of the thermal gas interaction elements T_0 is studied. The sensor is operated using CT mode at 100°C while T_0 is varied from 40°C to 70°C. Chamber pressure is set to the lowest point possible for the chamber, which is around $2 \cdot 10^{-7}$ mbar.

Fig. 3(a) shows a linear decrease of the sensor power against an increase in T_0. This result agrees with the linear relationship of sensor power and the temperature difference ΔT explained in Sec. 1.1.

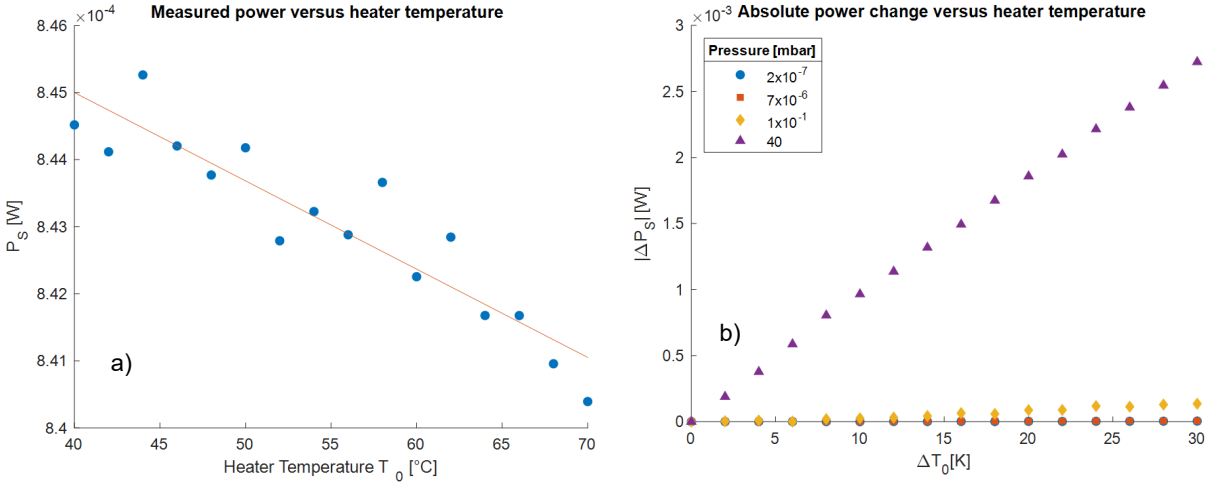

Fig. 3: a) Micro-wire Pirani power P_S versus thermal gas interaction elements temperature T_0 at base pressure $p_0 = 2 \cdot 10^{-7}$mbar; b) Absolute change in micro-wire Pirani power ΔP_S versus change in temperature T_0 at various pressures

The measurement is repeated at different chamber pressures. To visualize the degree of influence of ambient temperature on the power, the absolute difference of power $|\Delta P_S|$ is plotted against temperature change ΔT_0 in Fig. 3(b). ΔP_S is the difference of P_S relative to P_S at T_0 = 40°C and ΔT_0 is the temperature change relative to T_0 = 40°C.

As the chamber pressure increases, the difference in power due to the temperature change significantly increases. At $2 \cdot 10^{-7}$ mbar, the rate of $\Delta P_S/\Delta T_0$ is 0.13 µW/K whereas at 40 mbar the rate is 90.8 µW/K. This shows that the fluctuation in ambient temperature will affect the measurement accuracy more significantly in the higher pressure regimes compared to the lower pressure regimes. This also emphasizes the importance of ambient temperature stabilization for Pirani sensors.

For a stable PID control, we found out that the temperature difference between the micro-wire Pirani T_S and thermal gas interaction elements T_0 must be less than 10°C. Larger temperature differences will cause the PID control to fail especially at high pressures. After consideration of the upper voltage limit of the sensor, T_S = 90°C and T_0 = 85°C are found to be the most suitable for our system and will be used for the following experiments.

4.2. Comparison of measurement repeatability

To investigate the effect of temperature stabilization on measurement repeatability, measurements of pressure were performed in two cases: a) without temperature stabilization and b) with temperature stabilization. In both cases, the temperature of micro-wire Pirani T_S is 90°C whereas the temperature of thermal gas interaction elements T_0 is 85°C (for case (b) only). The measurements are repeated 4 times for both conditions

and the resulting micro-wire Pirani power P_S is measured from $1 \cdot 10^{-4}$ mbar to $2.5 \cdot 10^{2}$ mbar.

Fig. 4 shows P_S plotted against the pressure. From several insets, it can be seen that the single curves are much closer to each other for the case of temperature stabilization (orange curve) compared to the case of no temperature stabilization (blue curve). This becomes even more obvious in Fig. 5, where the standard deviation of P_S is plotted versus pressure. The graph shows that the measurement-to-measurement error is reduced significantly.

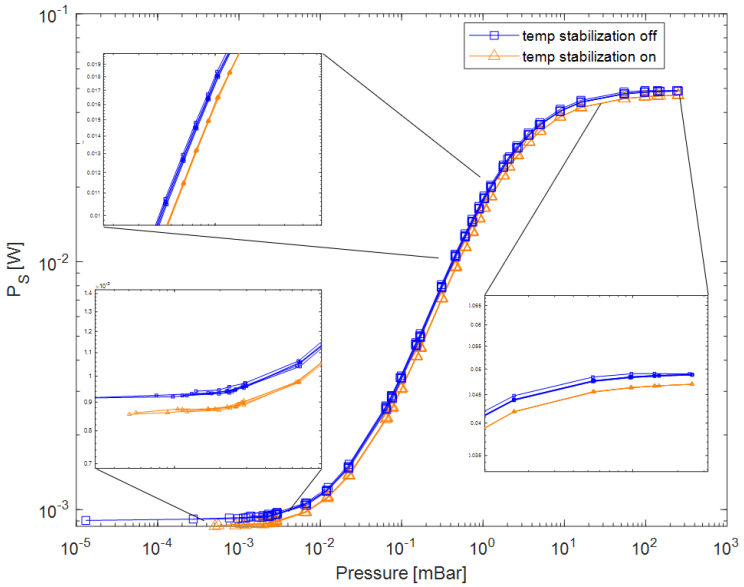

Fig. 4: Micro-wire Pirani power P_S measured against pressure with and without temperature stabilization.

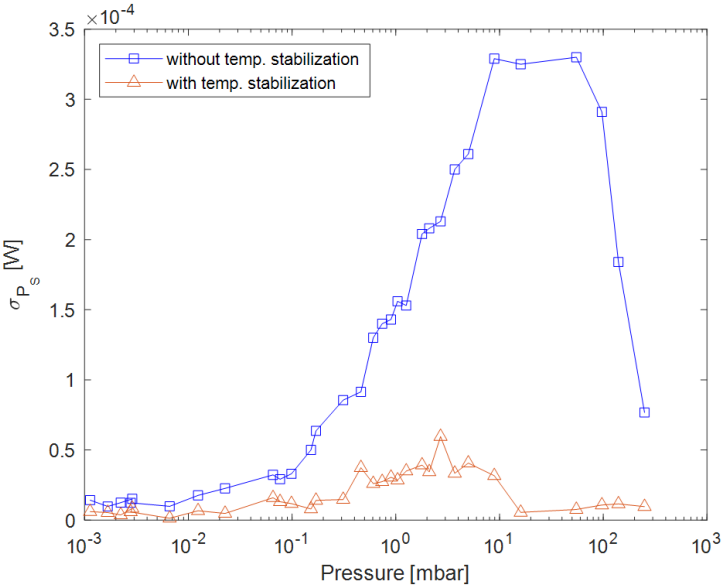

Fig. 5: Standard deviation of the micro-wire Pirani power P_S against pressure.

From Fig. 5 it also can be seen that the influence of the temperature fluctuation is much larger in the higher pressure regions, which is in agreement with Sec. 4.1. At its maximum point, the temperature-induced fluctuation in case of no temperature stabilization is 350 µW. In contrast, the temperature-induced signal fluctuations are kept at below 60 µW for the whole pressure range with temperature stabilization, which shows a significant reduction of about 83 %. These series of first measurements suggest that the thermal gas interaction elements work well to reduce the effect of the ambient temperature fluctuation and are crucial to increase measurement stability and repeatability.

5. Conclusion and outlook

In this work, we have introduced a new concept of ambient temperature stabilization of Pirani sensors. The temperature stabilization is obtained by an arrangement of thermal gas interaction elements made from thin zirconia to both sides of a Pirani micro-wire sensor.

Our micro-wire Pirani with a temperature-stabilized environment shows a reduction of temperature-induced signal fluctuations of up to 83 %. The optimal operating temperatures are 90°C and 85°C for the micro-wire and the thermal gas interaction elements respectively. We have also shown that the influence of ambient temperature on Pirani vacuum gauges' measurements will increase significantly with pressure. This emphasizes the importance of active temperature stabilization.

Ongoing work on this topic includes a study of long-term device stability, the comparison of different geometries, such as a variable distance between micro-wire Pirani and the thermal gas interaction elements, as well as further studies regarding the optimal operating parameters such as different temperature levels and power.

Acknowledgment

This work was supported by the German Federal Ministry of Education and Research under Project No. 13FH029KX0 (NEOVAK).

Literature

[1] Baklanov, Mikhail; de Marneffe, Jean-Francois et. al.: Plasma processing of low-k dielectrics. J. Appl. Phys. 113, 041101, 2013, pp.12-13.

[2] Reichelt, K.; Jiang, X.: The Preparation of Thin Films by Physical Vapour Deposition Methods. Thin Solid Films, 191, 1990, pp. 91-126.

[3] Danilatos, G. D.; Robinson, V. N. E.: SEM at High Specimen Chamber Pressures. Scanning Vol. 1´2, 2, 1979, pp. 72-82.

[4] Alvesteffer, W. J.; Jacobs, D. C.: Miniaturized thin-film thermal vacuum sensor. Journal of Vacuum Science & Technology A 13, 2980, 1995, pp. 2980-2981.

[5] Jitschin, W.: Gas Laws and Kinetic Theory of Gases, Handbook of Vacuum Technology. Wiley-VCH Verlag, 2016, p. 596.

[6] Berlicki, T. M.; Urbanski, K. J.: Ambient temperature effect in thin-film vacuum sensor. Vacuum 68, 2003, pp. 303-309.

[7] Shie, J. S.; Chou, C. S.: High-performance Pirani vacuum gauge. Journal of Vacuum Science & Technology A 13, 2972, 1995, pp. 2972-2979.

[8] Völklein, F.; Grau, M. et. al.: Optimized MEMS Pirani sensor with increased pressure measurement sensitivity in the fine and high vacuum regime. Journal of Vacuum Science & Technology A 31, 061604, 2013, pp. 3-5.

[9] Berlicki, T. M.: Thermal vacuum sensor with compensation of heat transfer. Sensors and Actuators A 93, 2001, pp. 27-32.

[10] Von Ubisch, H.: A New Hot-Wire Vacuum Gauge. Nature 161, 927-928, 1948.

[11] Berndt, D.: Muggli, J.; Heckel, R. et. al.: A Robust Miniaturized Gas Sensor for H_2 and CO_2 Detection Based on the 3w Method. Sensors 2022, 22, 485, pp. 1-3.

[12] Dams, F.: Schreiner, R.: Influencing factors on the sensitivity of MEMS-based thermal conductivity vacuum gauges. J. Vac. Sci. Technol. A 32(3), 2014, pp. 3-5.

[13] Jitschin, W.: 100 Jahre Pirani-Vakuummeter. Vakuum in Forschung und Praxis, 18 (6), 2006, pp. 22-23.

Kontakt

Mohd Fuad Rahiman
OTH Regensburg
Seybothstraße 2
93053 Regensburg
E-Mail: mohd.rahiman@st.oth-regensburg.de